

## Rigid Piles Under Inclined and Eccentric Loads

by

V.V.R.N. Sastry\*

G.G. Meyerhof\*\*

### Introduction

IN practice, piles are often subjected to combined action of horizontal and vertical loads coupled with moments. The ultimate resistance of a pile under horizontal load or pure moment was obtained based on an assumed lateral soil pressure distribution (Broms 1964, Meyerhof and Ranjan 1972). Lateral soil pressures from laboratory and field pile load tests are reported for the cases of pure moment and horizontal load (Adam, and Radhakaishna 1973 Briaud *et al.* 1983 Kerisel and Adam, 1967). Though the bearing capacity of piles in homogeneous soils under inclined eccentric loads has been earlier presented (Meyerhof and Yalcin, 1984, Meyerhof *et al.* 1983), the lateral soil pressures and the base resistance were not studied. However the, distribution of lateral soil pressures along a pile buried in sand and subjected to central inclined load has been reported (Chari and Meyerhof, 1983).

In continuation of the above work, pile tests on fully instrumented model piles have been carried out to study the variation of lateral soil pressures along the pile shaft with the total load on the pile, the carrying capacity of the pile and its base resistance. Piles were jacked into homogeneous soils and were subjected to central inclined and vertical eccentric loads.

### Model Tests

#### Soil Data

Dry silica sand of effective size  $D_{10} = 0.38$  mm and uniformity coefficient  $C_u = 2.8$  was used in the tests. The grains were angular with a texture and the initial porosity of sand was  $\eta = 47$  percent. This corresponds to a loose state with a relative density  $D_r = 0.2$ . From detailed

---

\*Research Associate, Technical University of Nova Scotia, Halifax, Nova Scotia, Canada, B3J 2X4.

\*\*Research Professor, Department of Civil Engineering, Technical University of Nova Scotia, Halifax, Nova Scotia, Canada, B3J 2X4.

(This paper was received in 1986 and is open for discussion till the end of September, 1987).

triaxial tests (Sastry, 1977) the angle of internal friction  $\phi_i$  at this porosity was about  $30^\circ$  while in plane strain value of  $\phi_p = 35^\circ$  was considered appropriate.

The clay used in the tests had a liquid limit  $W_L = 43$  percent, plastic limit  $W_p = 21.3$  percent, and water content  $W_n = 33$  percent having the degree of saturation,  $s_r$ , of about 98 percent. The average undrained shear strength of clay,  $c_u$ , was measured as 15 kPa from the unconfined tests carried out on samples obtained from the test beds.

### *Pile Data*

The vertical steel hollow pile was 1100 mm long, 74 mm in outside diameter with a 7 mm wall thickness. The pile was split longitudinally to facilitate instrumentation and the two halves were held together by ring connectors. In each tests, 18 pressure transducers were placed in the pile along the shaft, 9 on each half at the spacing of 74 to 148 mm to measure the lateral soil pressure. The total load applied through a hydraulic jack was measured by a proving ring and the vertical component of the base resistance was recorded by a load cell of 36 kN capacity. Eccentric loads were applied to a loading arm consisting of a steel box section  $100 \times 150$  mm which was firmly bolted to the pile cap. The displacements of the pile cap were measured by a series of dial gauges. The experimental setup is schematically shown in Fig. 1.

### **Test Details**

Sand was rained through a funnel from constant height into a corrugated steel drum about 1000 mm in diameter and 1600 mm high. The average sand density was found to be  $13.6 \text{ kN/m}^3$ . The clay was hand backed into a drum 600 mm in diameter and 1400 mm high. The pile was jacked at a rate of about 13 mm/min. to a depth of 950 mm and an axial load tests was conducted to verify the uniformity of soil layer in all the tests. After unloading, the pile test was immediately carried out with the load at the required inclination or eccentricity. A roller bearing was placed between the jack and the reaction frame to allow the movement of jack under load commensurate with displacement of the pile cap (Fig. 1). Two jacks, one vertical and the other horizontal, were used coupled with roller bearings to apply an inclined load. Pure moment was induced by two vertical jacks spaced 724 mm apart, one causing a downward force on the loading arm, while the other was causing an equal upward force through a yoke.

The failure of the pile was caused by loading in 10 to 12 equal increments and each load increment was maintained constant until the rate of displacement was less than 0.025 mm/min. in the case of piles in sand and less than 0.1 mm/min. in the case of piles in clay. Pile displacements, total load and base resistance were recorded for each load increment while

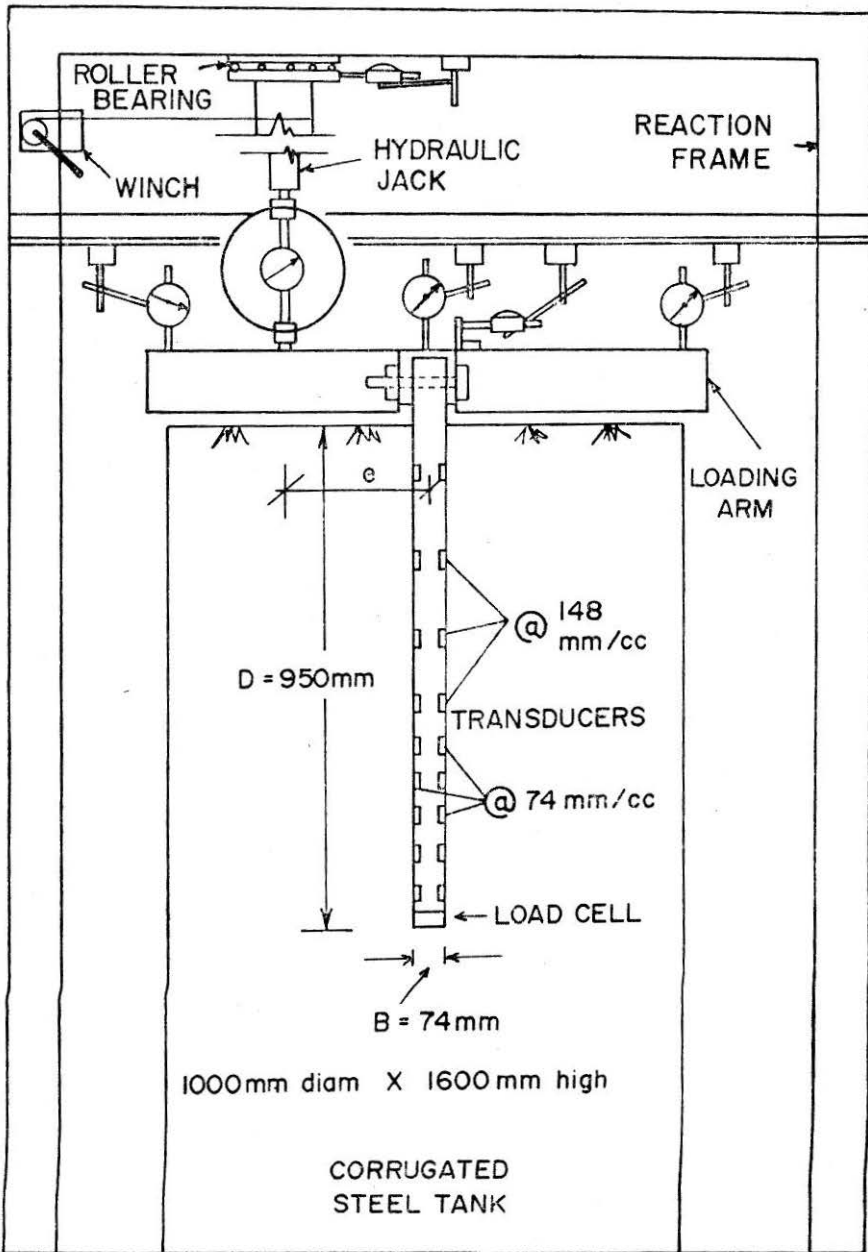


FIGURE 1. Schematic Diagram of Test Setup.

the lateral soil pressures were noted for alternate load increments. After the pile test in sand was completed, two static cone penetration tests were carried out, one on either side of the pile.

A total of six tests were carried out on the pile in sand, three under inclined loads and three under eccentric loads. The values of load inclination  $\alpha$  with the vertical were chosen as 30, 60, and 90°; while the ratios of eccentricity of load  $e$ /depth of pile  $D$ , were  $\frac{e}{D} = 0.16, 0.38, \text{ and } \infty$  (pure moment). In the case of pile in clay, six tests were conducted, two under inclined loads and four under eccentric loads. The values of load inclination chosen were  $\alpha = 45^\circ$  and  $90^\circ$ , while the values of eccentricities used were  $\frac{e}{D} = 0.16, 0.38, 1.17$  and  $\infty$ .

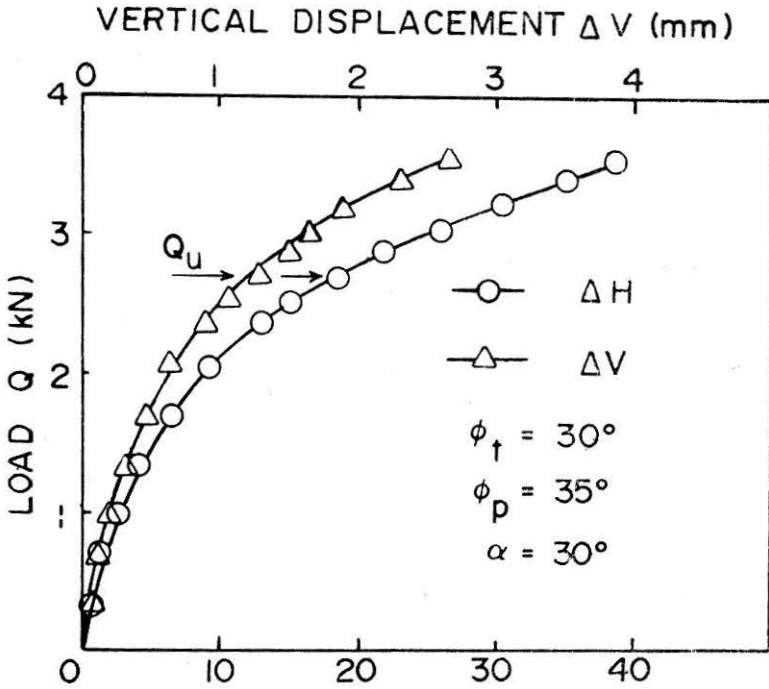
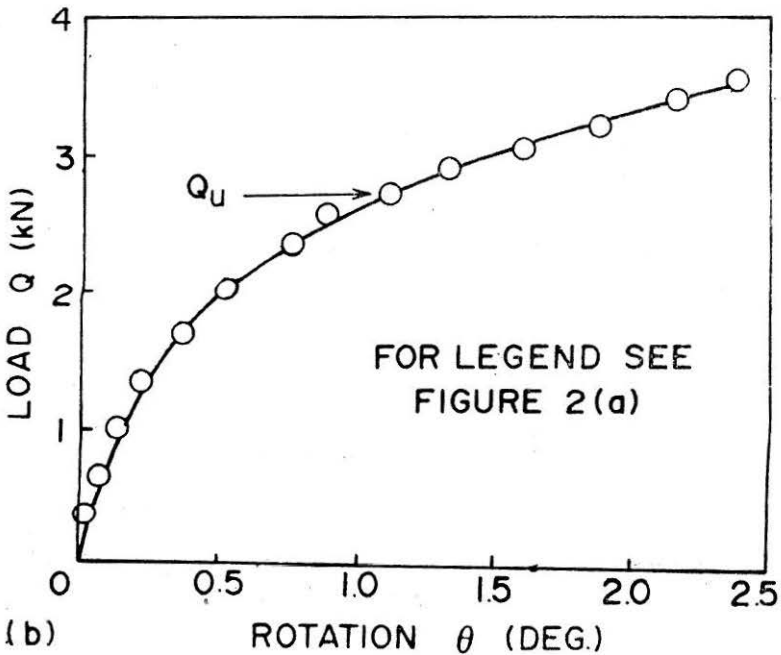
### Test Results

Typical load-displacement and moment-rotation curves for piles in sand and clay are shown in Figs. 2 and 3 respectively. The failure load or moment at which the increase in the displacement rate first reached its maximum was at a resultant pile displacement of about 0.5 — 3.5 percent of the pile length and occurred at a rotation of 1 — 2°.

The lateral soil pressure  $\sigma_i$  at any depth  $Z$ , due to the installation of pile in sand was negligible compared to lateral soil pressure  $\sigma$  due to the subsequent loading of the pile (Fig. 4). For selected cases of loading, the distribution of  $\sigma$  due to increasing inclined and eccentric loads on the pile are presented in Figs. 5 and 6, respectively.

However, in case of a pile jacked into clay, considerable lateral soil pressure is induced, as if the soil was prestressed due to installation (Fig. 4). Upon loading the pile, the  $\sigma_i$  value at any depth  $Z$  on the passive side was found to be increased by a value of  $\sigma_p$  while on the active side it was reduced by a value of  $\sigma_a$ . This phenomenon was observed both above and below the point of rotation along the pile. The  $\sigma_p$  and  $\sigma_a$  values at any depth are numerically added to obtain the net lateral soil pressure  $\sigma$  due to loading of the pile. The distribution of this net pressure  $\sigma$  with depth at different loads, for typical inclinations and eccentricities of load are shown in Figs. 7 and 8, respectively.

For piles under inclined loads, the ultimate load  $Q_u$  and the corresponding base resistance  $Q_p$  are presented in Figs 9 (a) and (b) for sand and clay, respectively, using polar bearing capacity diagrams. In the case of piles under eccentric loads, the load eccentricity  $e$  is converted into an equivalent inclination  $\theta$  where  $\theta = \tan^{-1} e/D$ . The failure load  $Q_u$  is plotted as ordinate, while  $M_u/D$  is plotted as abscissa for sand and clay in Figs 10 (a) and (b), respectively ( $M_u = Q_u.e$ ).

(a) HORIZONTAL DISPLACEMENT  $\Delta H$  (mm)

(b)

FIGURE 2. Typical Results of Model Pile in Sand under Inclined Load  
 (a) Load-Displacements (b) Load-Rotation.

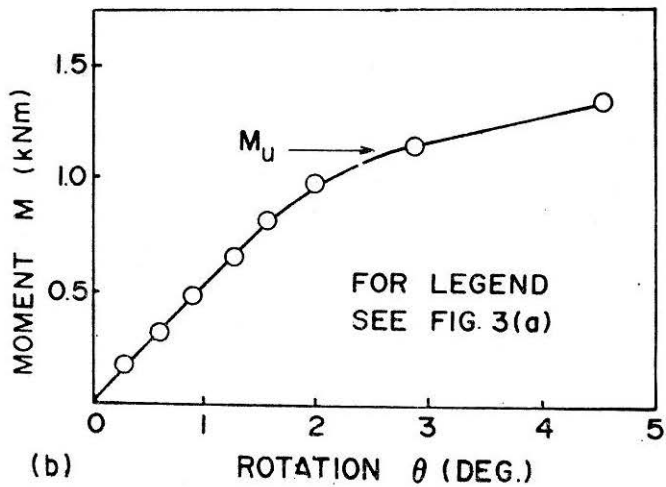
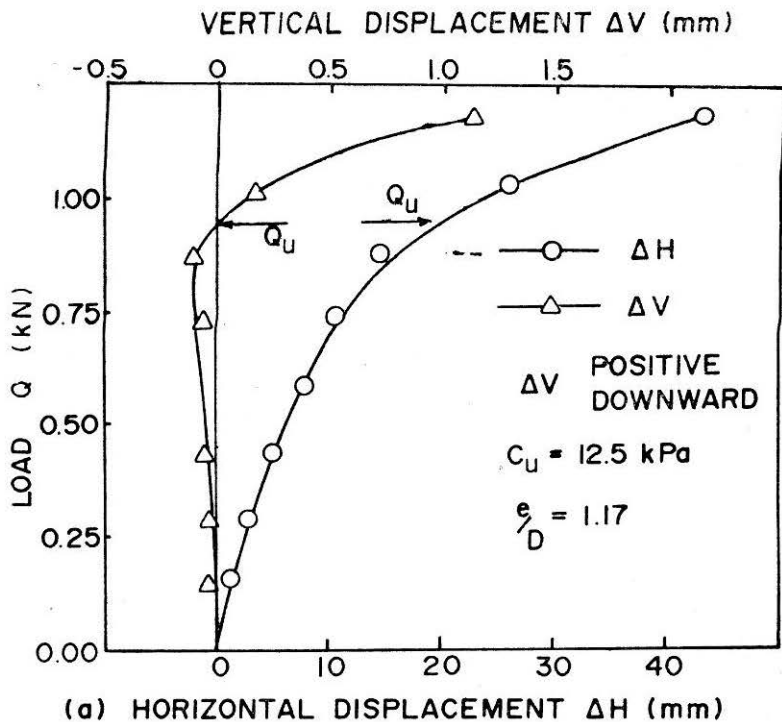


FIGURE 3 Typical Results of Model Pile in Clay under Eccentric Load  
 (a) Load-Displacements (b) Moment-Rotation.

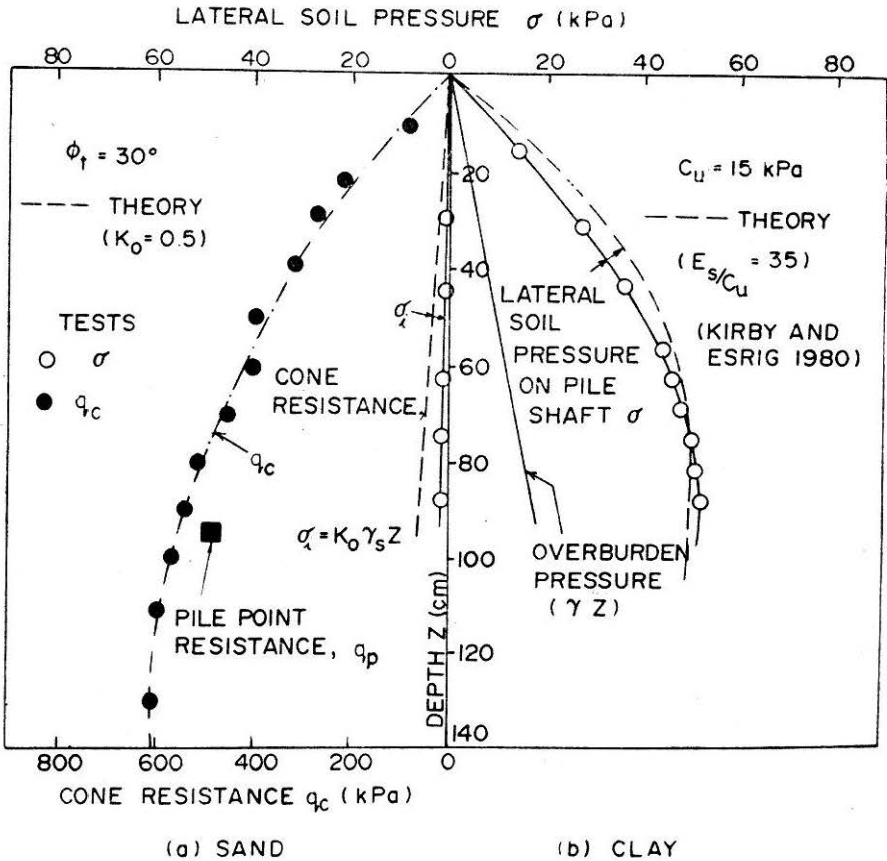


FIGURE 4 Lateral Soil Pressures due to Pile Installation and Results of Cone Penetration Tests.

Since the lateral soil pressures were measured for alternate load increments, the ultimate loads and moments stated in Figs 7 and 8 for some cases are slightly different from the failure loads and moments shown in Figs 9 and 10.

### Analysis of Test Results

#### Pile in Sand

#### Lateral Pressures

When a fully embedded rigid pile is acted upon by a central inclined load or an eccentric vertical load  $Q_u$ , the lateral soil pressure  $\sigma$  at failure is approximately represented by triangular distribution (Fig. 11 (a)). The forces  $P_1$  and  $P_2$  are inclined at  $\delta_1$  and  $\delta_2$  while the point resistance  $Q_p$  is inclined at  $\delta_3$ . The vertical component of  $Q_p$  is measured by the load cell while the horizontal component is obtained from the equilibrium considerations. The value of  $\sigma_i$  at any depth  $Z$  due to the pile installation may be

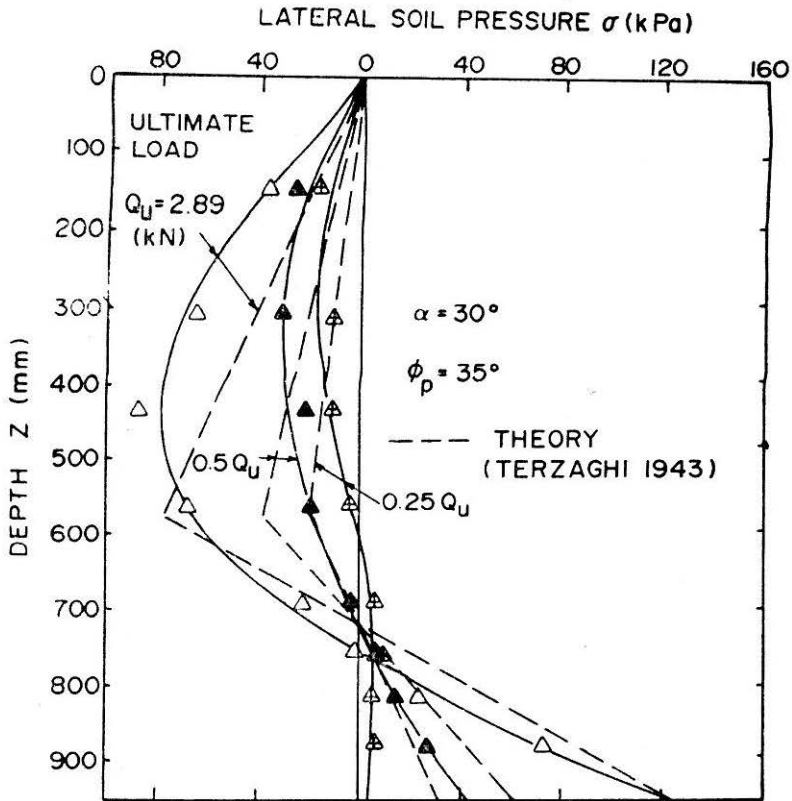


FIGURE 5(a) Variation of Lateral Soil Pressure with Applied Load in Case of Pile in Sand under Inclined Loads at  $\alpha = 30^\circ$

estimated from  $\sigma_i = K_o \cdot \gamma \cdot Z$ , in which  $K_o = 1 - \sin \phi_i$  and  $\gamma$  = density of the soil. The measured  $\sigma_i$  value due to the pile installation are found to be much less compared to the estimates (Fig. 4) and are seen to be insignificant when compared to the  $\sigma$  values induced due to subsequent loading of the pile. As a result, the effect of pile installation is neglected in the further analysis.

For the purpose of computing the pile capacity, the distributions of net lateral soil pressure at failure due to a horizontal load or pure moment can be roughly estimated by the triangular distribution suggested by Terzaghi (1943). The magnitude of the lateral soil pressure at shallow depth is obtained from earth pressure theory incorporating a shape factor while at the base of pile it is obtained by considering the bearing capacity of a vertical semicircular strip footing at depth. Reasonable agreement is noticed between the observed and estimated values of  $\sigma$  at failure (Figs. 5 and 6(b)). The effect of increasing total load  $Q$  on the magnitude of  $\sigma$  at any depth is analysed by examining the measured  $\sigma$  values under working loads (Figs. 5 and 6). The maximum lateral soil



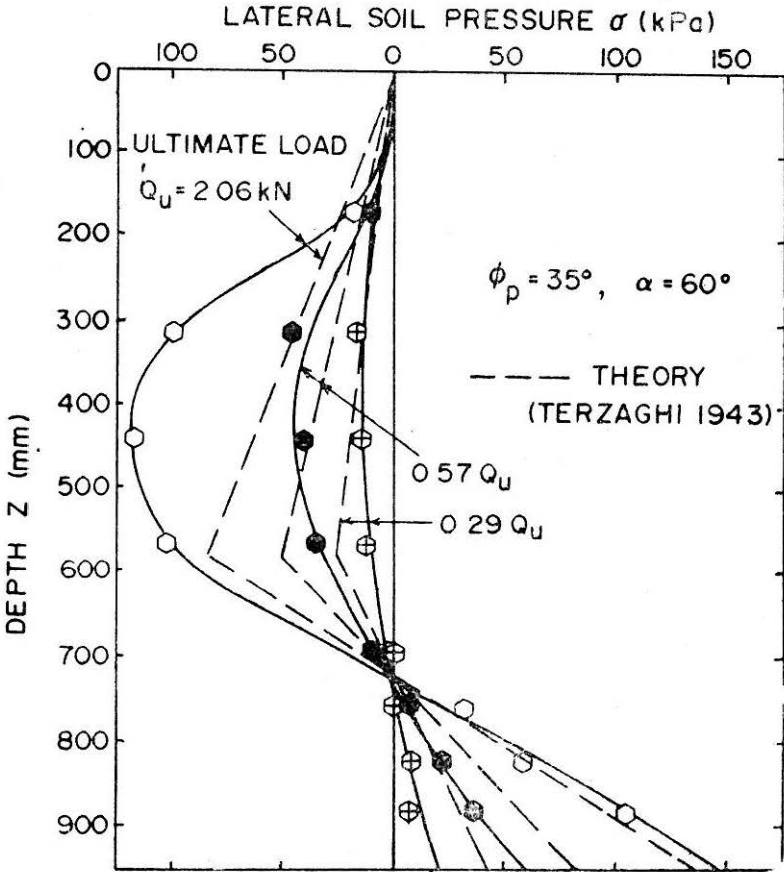


FIGURE 5(b) Variation of Lateral Soil Pressure with Applied Load in Case of Pile in Sand under Inclined Loads at  $\alpha = 60^\circ$ .

pressures ( $\sigma_1$  and  $\sigma_b$ ), the horizontal components of earth thrusts ( $P_1$  and  $P_2$ ) on the pile above and below the point of rotation, under a given load  $Q$  (Fig. 11(a)) are seen to be approximately linearly varying with the load  $Q$ . Typical values of  $\sigma/\sigma_u$  at salient points along the shaft were plotted on the abscissa with corresponding values of  $Q/Q_u$  plotted as ordinates,  $\sigma_u$  and  $Q_u$  representing values at failure. Most of the points were seen to fall along the  $45^\circ$  line through origin indicating a linear relation between  $Q$  and  $\sigma$  (Sastry and Meyerhof, 1986). Thus, the theoretical lateral soil pressure distribution, due to an ultimate horizontal load or pure moment, can roughly be linearly stepped down in proportion to the load or moment, in order to arrive the distribution under corresponding working loads. However, this linearisation is seen to be valid only up to a factor of safety of about  $F \leq 2$  where  $F = Q_u/Q$ . For intermediate inclinations and eccentricities, the ultimate  $\sigma_b$  value at the pile base can be estimated from Figs. 9(a) and 10(a), as will be explained in the next section. The  $\sigma$  distribution under working loads can be obtained proportionate to the

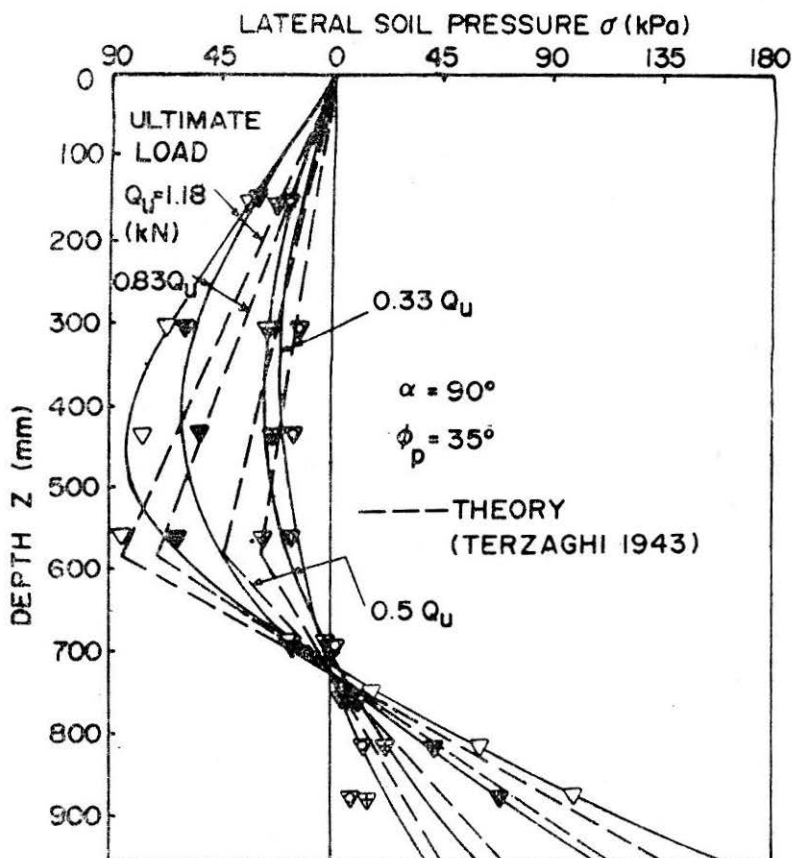


FIGURE 5 Variation of Lateral Soil Pressure with Applied Load in Case of Pile in Sand under Inclined Loads at  $\alpha = 90^\circ$ .

load on the pile. Reasonable agreement is noticed between the estimated and observed values of  $\sigma$  for the two types of loading investigated (Figs. 5 and 6).

The depth of point of rotation, where the  $\sigma$  value is zero, is seen to agree closely with the estimated value for both inclined and eccentric loads. This depth is greater in the case of inclined loads when compared to eccentric loads as would be expected theoretically (Figs. 5 and 6). The actual pattern of lateral soil pressure distribution is quite complicated. It is seen to depend not only on the load level but also on the inclination or eccentricity of the load. The point of rotation seems to move downwards with increasing load for a given inclination or eccentricity of the load. Thus, the lateral pressure distribution suggested by Terzaghi (1943) seems to hold promise in the case of a pile under pure horizontal load or moment at failure.

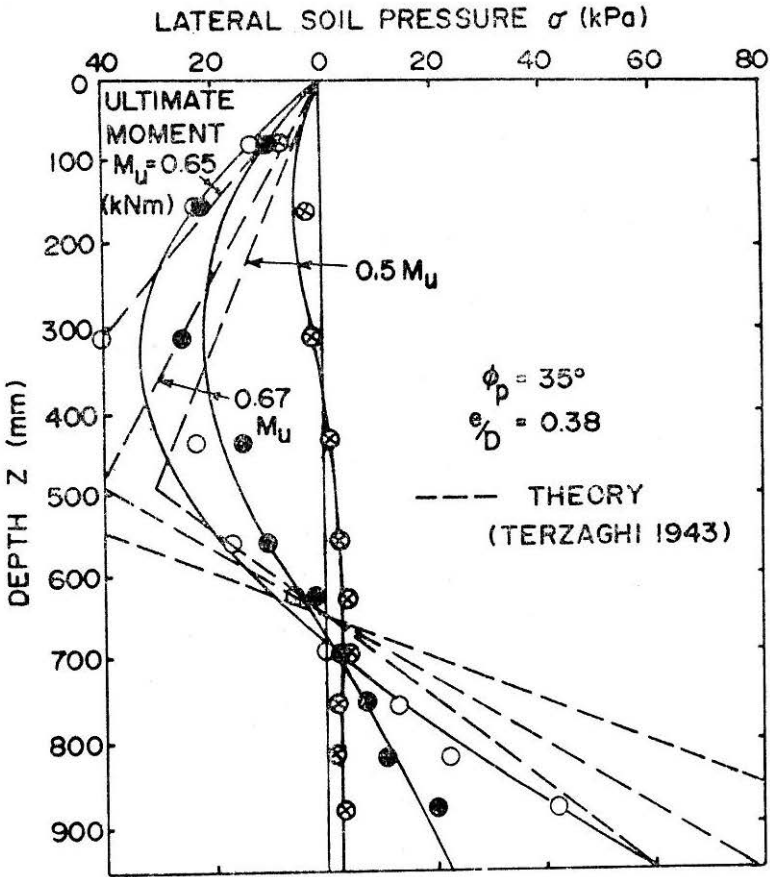


FIGURE 6(a) Variation of Lateral Soil Pressure with Applied Load in Case of Pile in Sand under Eccentric Loads for  $e/D = 0.38$ .

*Bearing Capacity*

The pile capacity under inclined load is bounded by two extremes of the axial and lateral capacities of the pile. The axial capacity  $Q_o$  is obtained from conventional bearing capacity theory (Meyerhof, 1976).

$$Q_o = \gamma \cdot D \cdot N_q \cdot A_p + \frac{1}{2} \cdot \gamma \cdot DK_s \tan \delta A_s \quad \dots (1)$$

in which  $N_p$  = Bearing capacity factor,  $A_p$  and  $A_s$  are the areas of pile point and shaft respectively,  $\delta$  = Friction angle between soil and pile,  $K_s$  = Average coefficient of earth pressure on pile shaft and the other symbols as before. The pile capacity  $Q_{90}$  under a horizontal load is obtained from the equilibrium considerations, assuming a smooth pile ( $\delta_1 = \delta_2 = 0$ ) so that

$$Q_{90} = 0.12 K_b \gamma B D^2 \quad \dots (2)$$

$$= 0.12 \sigma_b B \cdot D \text{ where } \sigma_b = K_b \cdot \gamma D; \quad \dots (3)$$

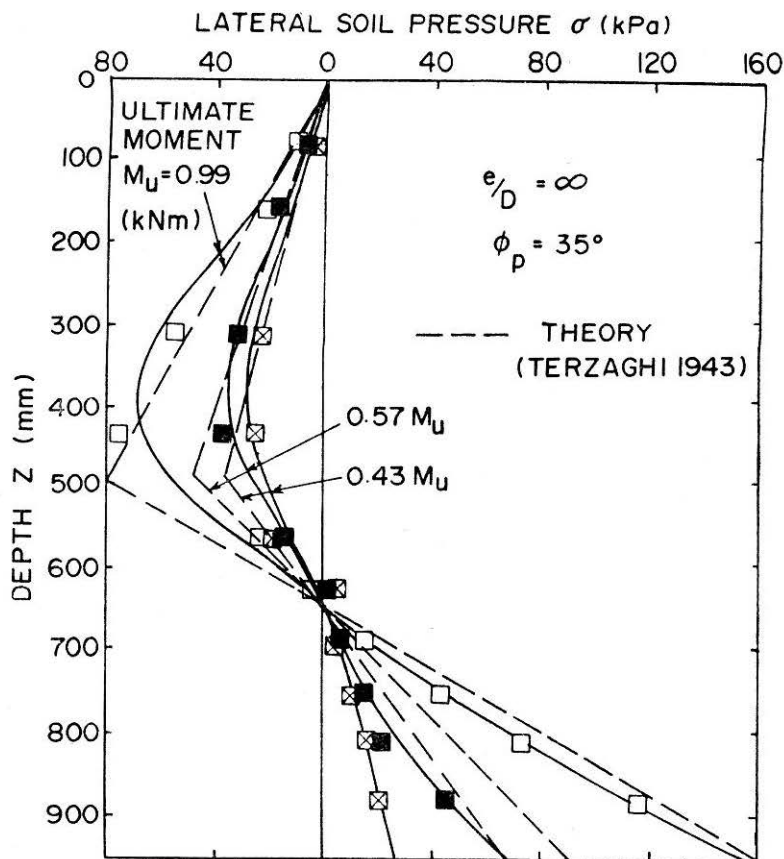


FIGURE 6 Variation of Lateral Soil Pressure with Applied Load in Case of Pile in Sand under Eccentric Loads for  $e/d = \infty$ .

$B$  = Diameter of pile,  $K_b$  = Lateral earth pressure coefficient for pile (Meyerhof *et al.* 1981).

For any intermediate inclination  $\alpha$ ,  $Q_u$  may be obtained by using the inclination factor (Koumoto *et al.* 1986), so that

$$Q_u = Q_o \left[ 1 - \left( 1 - \frac{Q_{90}}{Q_o} \right) \sin \alpha \right] \quad \dots (4)$$

The shaft friction  $\delta$  was seen to be  $0.6 \phi_p$  in the case axial load while  $\delta = 0$  was mobilized under horizontal load. For intermediate inclinations, a linear variation of  $\delta$  may be adopted to estimate  $Q_u$  from Eq. (4) in which  $Q_{90}$  was computed with a  $K_b$  value appropriate to the  $\delta$  mobilized for that inclination.

The observed values of  $Q_u$ , when compared with the estimates based on

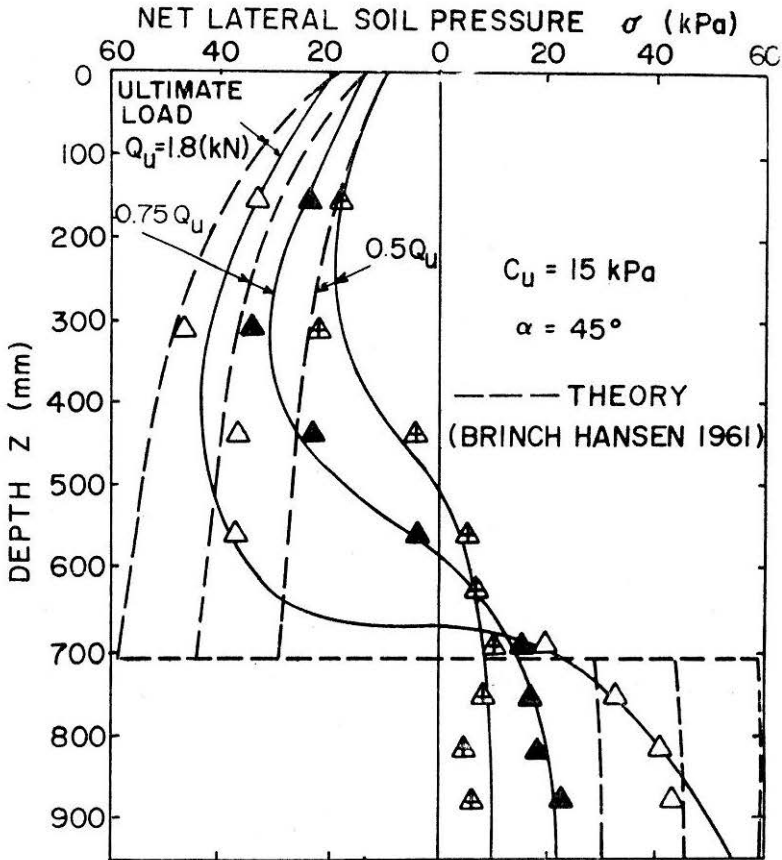


FIGURE 7(a) Variation of Net Lateral Soil Pressure with Applied Load in Case of Pile in Clay under Inclined Loads at  $\alpha=45^\circ$ .

a value of  $\phi_p = 35^\circ$  indicate that the theory is on the side of safety (Fig. 9(a)). Since  $Q_{90}$  is also expressed in terms of  $\sigma_b$  (Eq. 3) and  $\sigma_b$  value is linearly related to  $Q$ , the curve for  $Q_u$  in Fig. 9(a) can also be used to estimate ultimate  $\sigma_b$  for any intermediate inclination  $\alpha$  of the load.

The pile capacity under an eccentric load is bounded by the axial and pure moment capacities of the pile. The maximum pure moment at failure  $M_o$  is obtained by assuming a smooth pile ( $\delta_1 = \delta_2 = 0$ ) and setting  $P_1 = P_2$  so that

$$M_o = 0.083 K_b \cdot \gamma \cdot BD^3 \quad \dots (5)$$

$$= 0.083 \sigma_b BD^3 \text{ with symbols as before; } M_o \text{ can also be expressed in terms of } Q_{90} \text{ as} \quad \dots (6)$$

$$M_o = m Q_{90} D \text{ where } m = 0.7 \quad \dots (7)$$

The pile capacity under a given eccentricity  $e$  can be expressed in terms of the eccentricity factor (Koumoto *et al.* 1986).

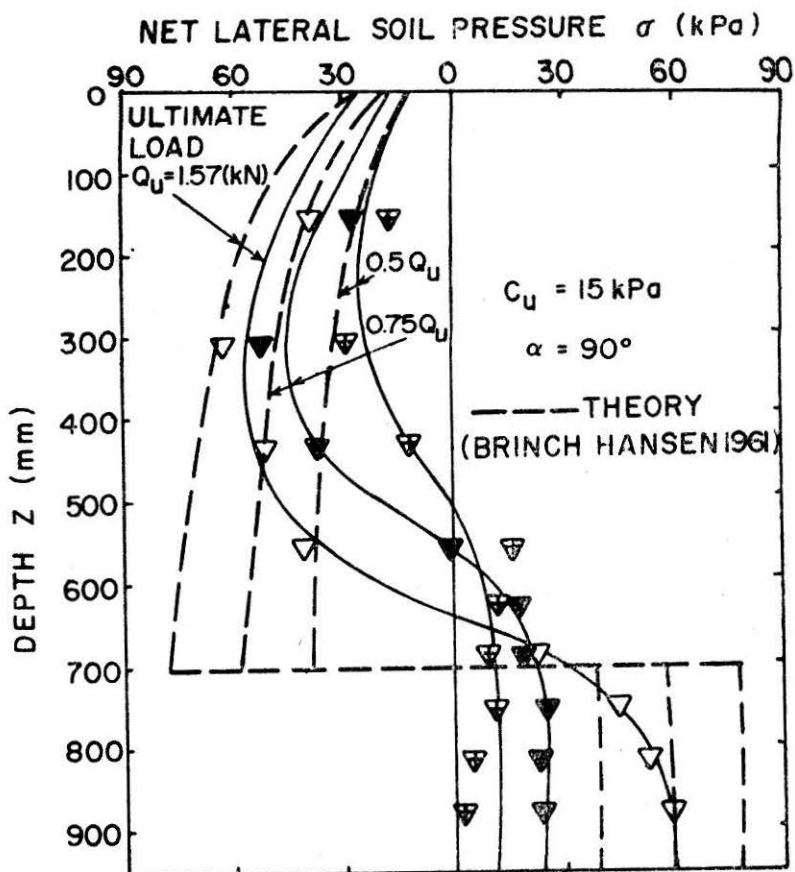


FIGURE 7 Variation of Net Lateral Soil Pressure with Applied Load in Case of Pile in Clay under Inclined Loads at  $\alpha = 90^\circ$ .

$$Q_u = Q_o \cos \theta \left[ 1 - \left( 1 - \frac{m Q_{90}}{Q_o} \right) \sin \theta \right] \quad \dots (8)$$

where  $\theta = \tan^{-1} \left( \frac{e}{D} \right) \quad \dots (9)$

In estimating  $Q_u$  values from Eq. (8), for intermediate eccentricities, a linear interpolation of  $\delta$  value between  $0.6 \phi_p$  for the axial case and zero for the pure moment case is suggested when computing an appropriate  $Q_{90}$  for the mobilized  $\delta$ . It is seen that the predicted values  $Q_u$  are in good agreement with the observed values (Fig. 10(a)). Once again, since  $M_o$  is expressed in terms of  $\sigma_b$  (Eq. 6), the curve of  $Q_u$  in Fig. 10(a) can also be used to estimate the  $\sigma_b$  values for intermediate eccentricities of the load.

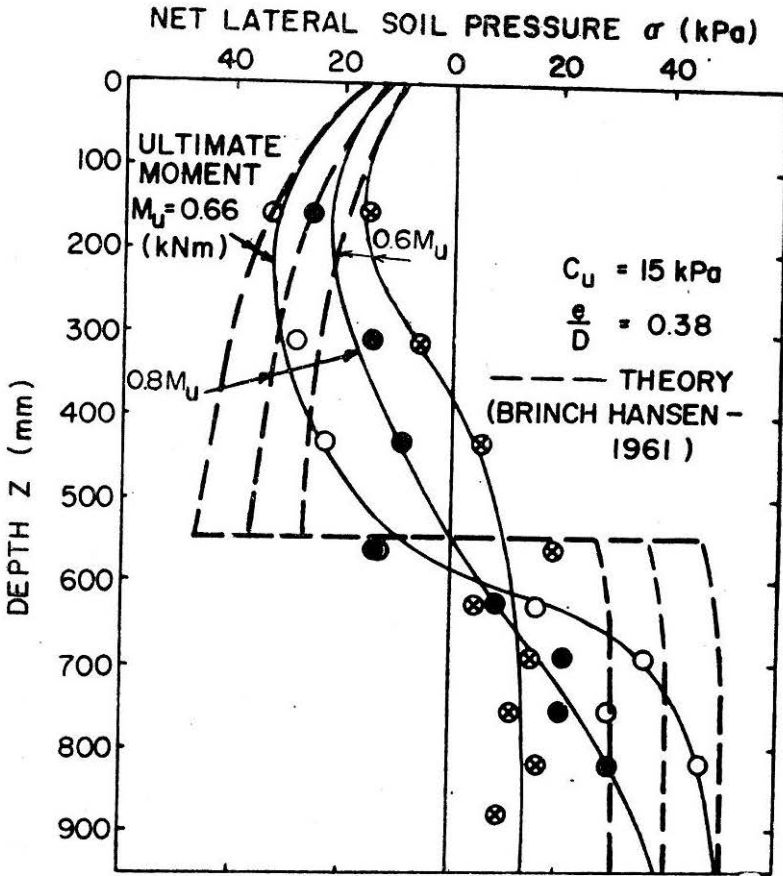


FIGURE 8(a) Variation of Net Lateral Soil Pressure with Applied Load in Case of Pile under Eccentric Loads for  $e/D = 0.38$ .

The variation in the magnitude and inclination of the base resistance  $Q_p$  with increasing total load  $Q$  on the pile was analysed.  $Q_p$  was seen to vary approximately linearly with  $Q$  while its inclination  $\delta_3$  changed roughly linearly from about  $-\phi_t$  to  $+\phi_t$  as  $Q/Q_u$  changed from 0 to 1. The value of  $Q_p$  under axial load is given by the first part of Eq. (1). In case of inclined or eccentric loads, its value can be readily obtained from the inclination factor  $i_\gamma$  (Meyerhof and Hanna, 1978). The estimated values of  $Q_p$  are safe when compared to the observed values (Fig. 9(a)).

### Pile in Clay

#### Lateral Pressures

When a rigid pile embedded in clay is subjected to an inclined or eccentric load  $Q_u$ , the lateral soil pressure at failure is approximately represented by the roughly rectangular distribution (Fig. 11(b)). Apart from the earth thrusts  $P_1$  and  $P_2$ , soil adhesions  $C_1$  and  $C_2$  are mobilized

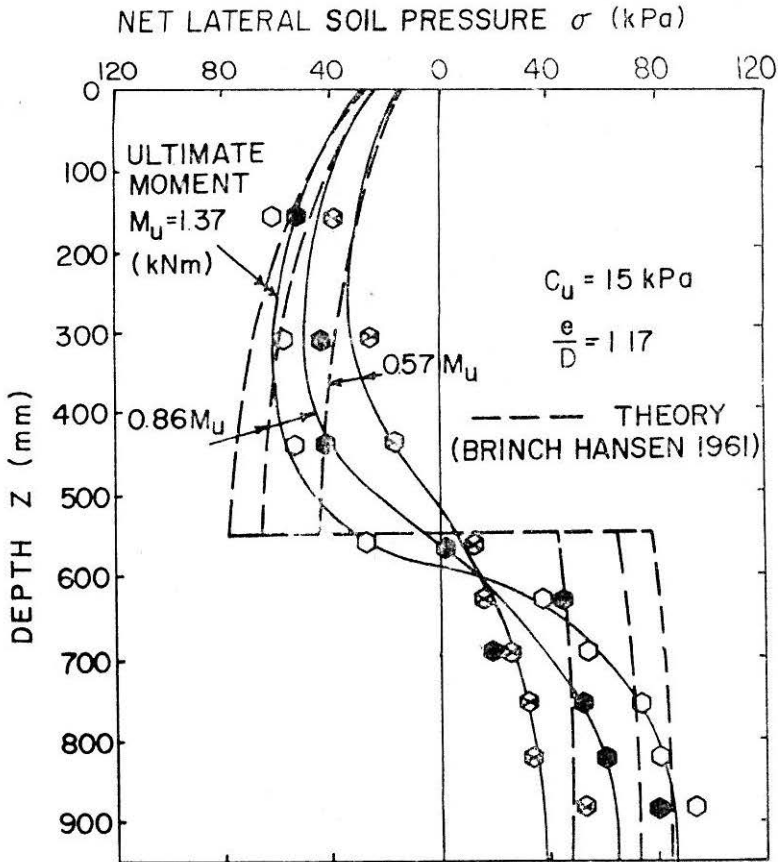


FIGURE 8(b) Variation of Net Lateral Soil Pressure with Applied Load in Case of Pile in Clay under Eccentric Loads for  $e/D=1.17$ .

along the shaft with the tip resistance  $Q_p$  inclined at  $\delta_3$ . Due to the jacking of pile into the clay, considerable lateral soil pressures are developed on the pile shaft. The theoretical estimate of this soil pressure in the present tests is  $\sigma_i = 3.3 c_u$ . This estimate is obtained for the value of  $E_s/C_u = 35$  (Kirby and Esrig, 1980), where  $E_s =$  Secant modulus and  $C_u =$  Undrained strength of the soil. Assuming a parabolic variation of  $\sigma_i$  from zero at the surface to its maximum value at a depth of  $10 B$ , reasonable agreement is noticed between the observed and estimated values of  $\sigma_i$  (Fig. 4).

From the observed lateral soil pressures along the shaft of a pile subjected to a horizontal load or pure moment, the distribution of  $\sigma$  suggested by Brinch Hansen (1961) was seen to hold promise. The theoretical estimate of  $\sigma$  values at failure is based on the earth pressure coefficients (Meyerhof, 1972), allowing 80 percent of the values proposed for rough piles to account for the smoothness of the shaft in the present tests. Once



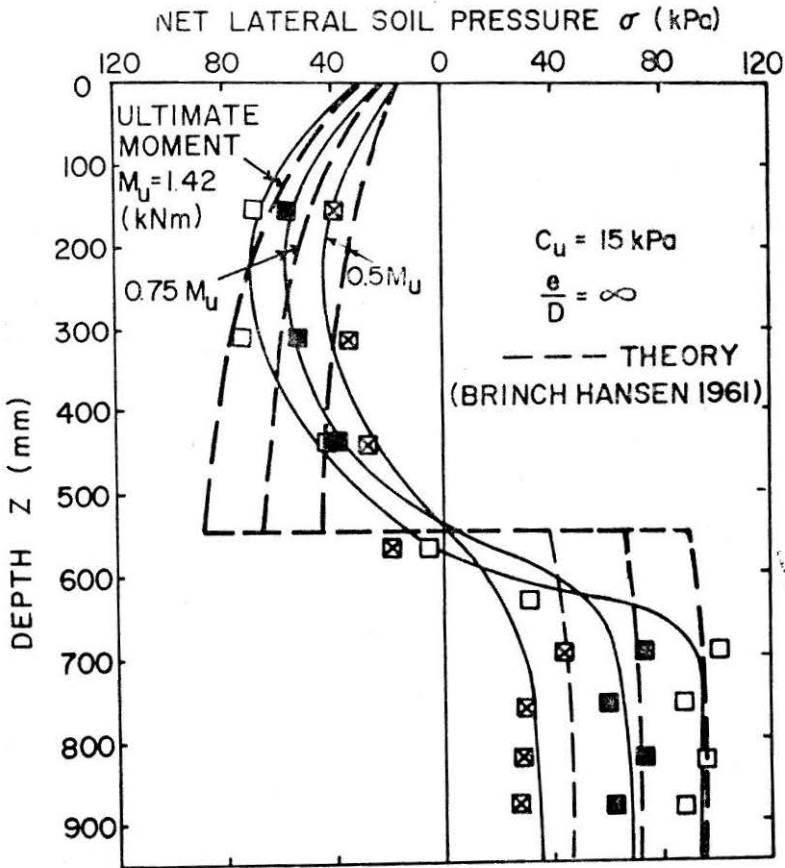


FIGURE 8(c) Variation of Net Lateral Soil Pressure with Applied Load in Case of Pile in Clay under Eccentric Loads for  $e/d = \infty$ .

again, the effect of increasing load on the  $\sigma$  value is analysed by examining the measured  $\sigma$  values under increasing load or moment at salient points along the shaft. Although the  $\sigma$  is not precisely linearly varying with the load  $Q$ , a linear relation may safely be assumed between  $Q$  and  $\sigma$  (Sastri and Meyerhof, 1986). Thus, the theoretical pressure distribution  $\sigma$  at ultimate horizontal load or pure moment may be linearly reduced proportionate to the load or moment in order to arrive at the  $\sigma$  distribution under corresponding working loads up to about  $F \leq 2$ . For intermediate inclinations and eccentricities of the load, the lateral soil pressure at pile base  $\sigma_b$  value can be estimated from Fig. 9(b) and 10(b) respectively.

When compared with the measured values, the estimated values of  $\sigma$  are seen to be on the safe side (Figs. 7 and 8).

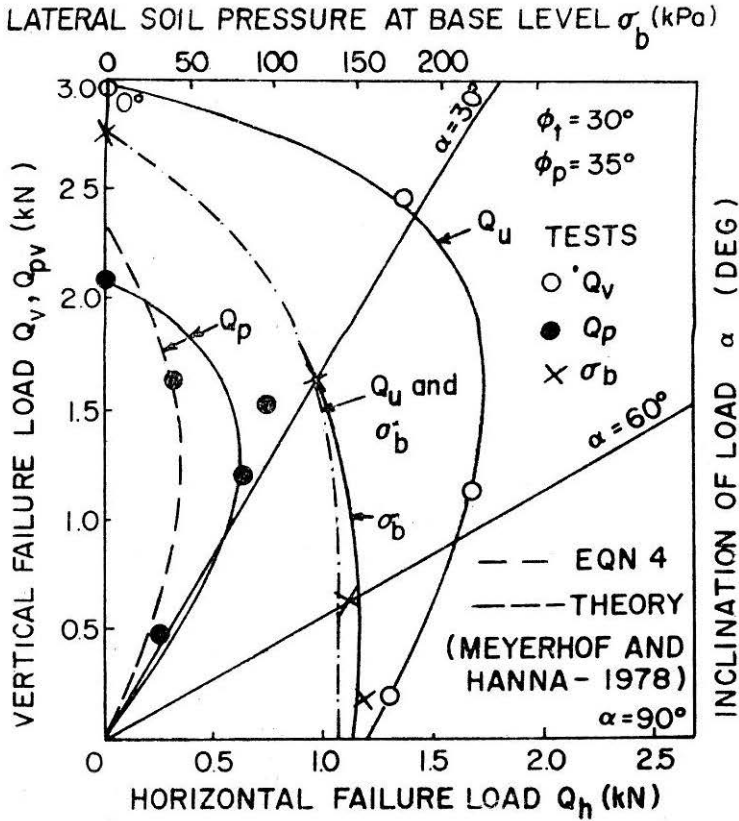


FIGURE 9(a) Polar Bearing Capacity Diagram for Pile under Inclined Loads in Sand.

*Bearing Capacity*

The pile capacity under axial load is obtained theoretically from:

$$Q = 9 c_u A_p + r c_u A_s \quad \dots (10)$$

Where  $r$  = adhesion factor and other symbols as before. The  $Q_{90}$  under a horizontal load can be obtained by considering the equilibrium of the smooth pile (Fig. 11(b)) so that

$$Q_{90} = 0.4 K_c \left( 1 - 5 \frac{B}{D} \right) c_u B D \quad \dots (11)$$

$$= 0.4 \sigma_b \left( 1 - 5 \frac{B}{D} \right) B \cdot D \quad \dots (12)$$

Since  $\sigma_b = K_c \cdot c_u$

Where  $K_c$  = Earth pressure coefficient for smooth pile (Meyerhof *et al.*, 1981). For intermediate inclinations the pile capacity  $Q_u$  and the net

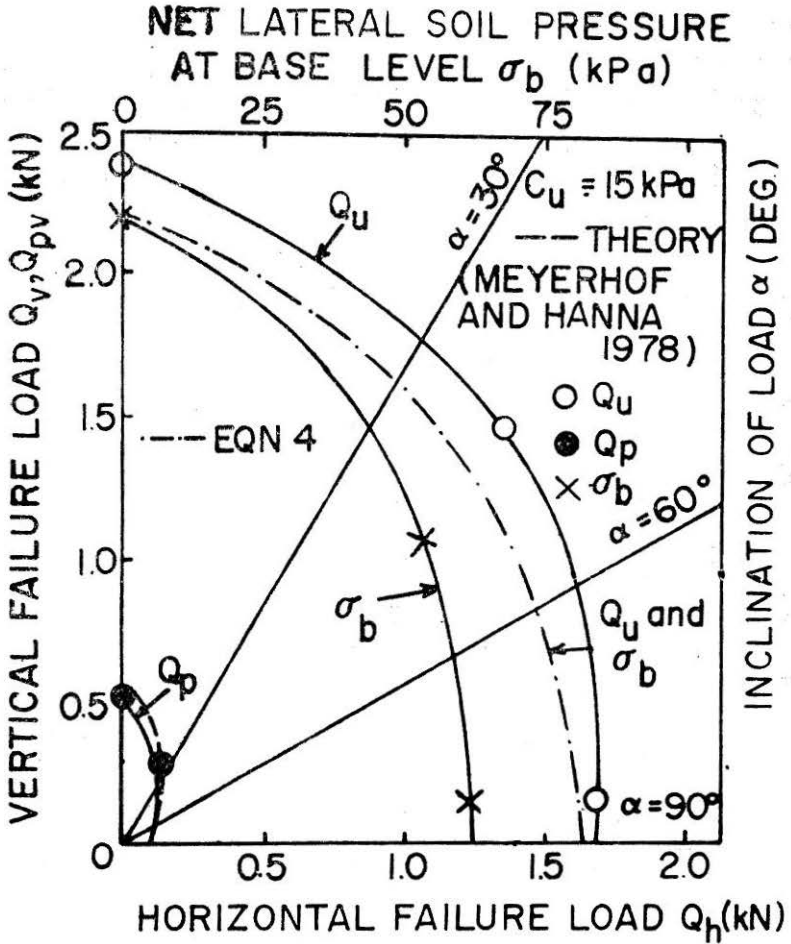


FIGURE 9(b) Polar Bearing Capacity Diagram for Pile under Inclined Loads for Clay.

lateral pressure at the pile base  $\sigma_b$  can be approximately estimated using Eq. (4). The estimated values of  $\sigma_b$  and  $Q_u$  are on the safe side compared to the measured values (Fig. 7 and 9(b)).

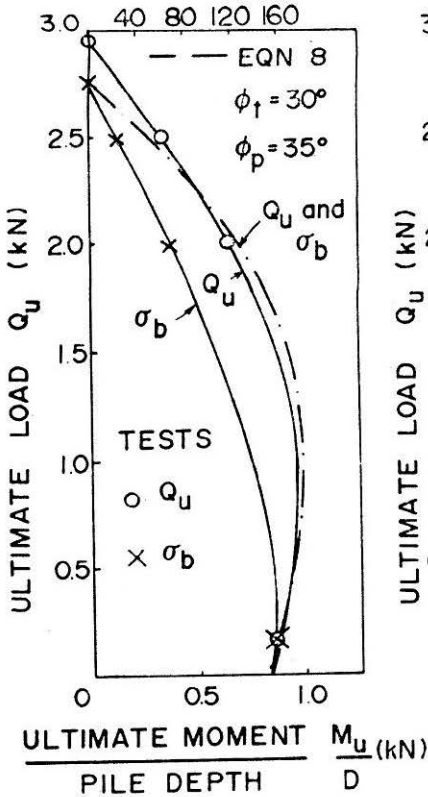
The maximum pure moment at failure  $M_o$  is once again obtained from the equilibrium considerations of the smooth pile.

Thus,

$$M_o = 0.25 K_c c_u B D^2 \left( 1 - 4 \frac{B}{D} \right) \quad \dots (13)$$

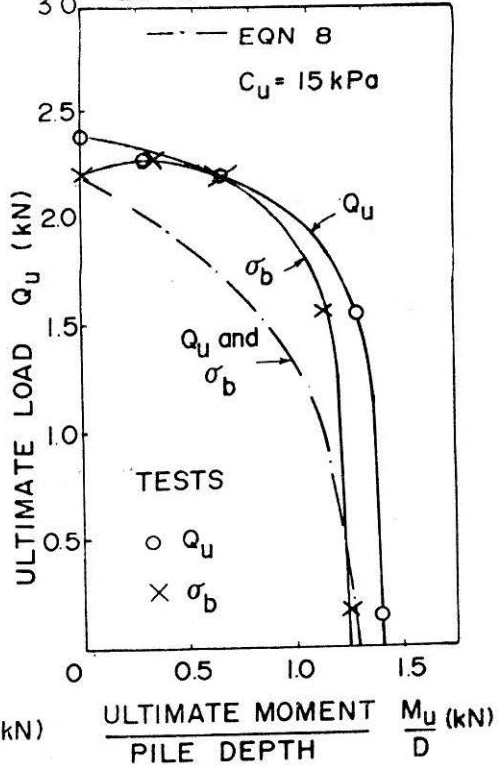
$$= 0.25 \sigma_b B D^2 \left( 1 - 4 \frac{B}{D} \right) \text{ with symbols as before} \quad \dots (14)$$

LATERAL SOIL PRESSURE  
AT PILE BASE.  $\sigma_b$  (kPa)



(a)

NET LATERAL SOIL PRESSURE  
AT PILE BASE  $\sigma_b$  (kPa)



(b)

FIGURE 10 Interaction Diagram between Ultimate Load and Moment for Pile under Eccentric Loads (a) Sand (b) Clay.

$M_0$  can also be expressed in terms of  $Q_{90}$  using Eq. (7), where  $m = 0.6 \left( 1 + \frac{B}{D} \right)$ . Thus, the pile capacity under intermediate eccentricity can be estimated from Eq. (8).

As explained earlier, the curve for  $Q_u$  in Fig. 10(b) also estimates the  $\sigma_b$  at failure for a given eccentricity of the load. The estimated values of  $Q_u$  and  $\sigma_b$  are on the side of safety compared to the observed values. The value of  $Q_p$  under axial load is given by the first part of Eq. (10) and in case of inclined or eccentric loads its value can be readily obtained from the inclination factor  $i_e$  (Meyerhof and Hanna, 1978). Close agreement is seen between estimated and observed values of  $Q_p$  (Fig. 9(b)).

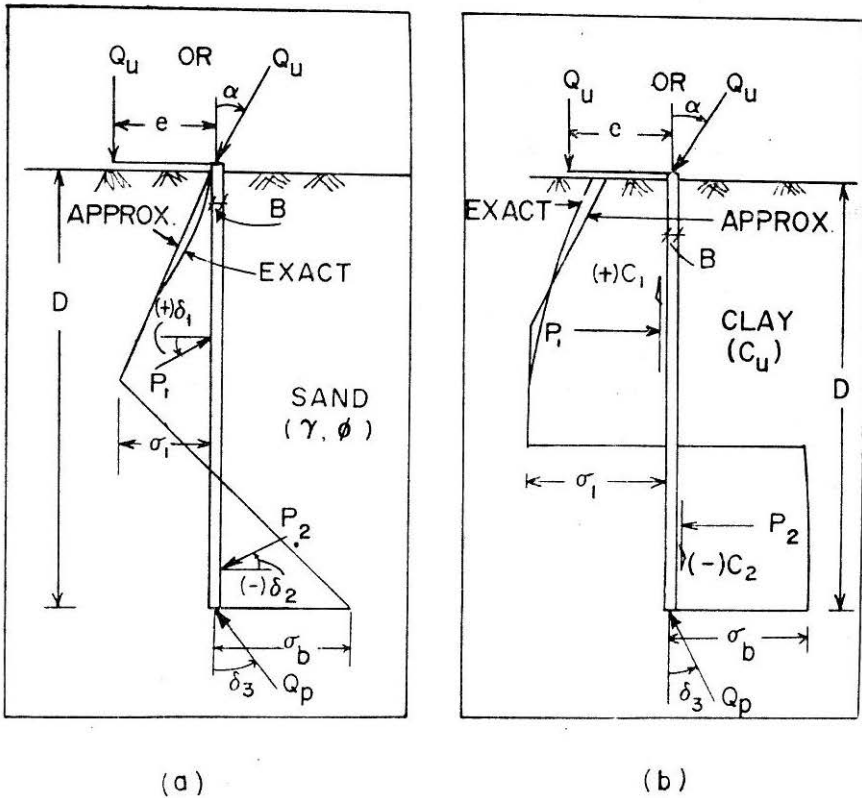


FIGURE 11 Forces at Failure of Pile under Inclined or Eccentric Load (a) Sand (b) Clay.

### Conclusions

Analysis of observed lateral soil pressures along the pile shaft and the point resistance of piles jacked into homogeneous sand and clay, subjected to central inclined and vertical eccentric loads have lead to an understanding of their variation with the applied load. The ultimate pile capacity under horizontal load pure moment can be estimated based on the observed lateral soil pressure variation. For intermediate inclination or eccentricity of the load, the pile capacity and the lateral soil pressure at the base of pile can be roughly estimated from the inclination or eccentricity factors suggested earlier.

Triangular distribution of lateral pressures suggested by Terzaghi (1943) seems to be valid for piles in sand while the roughly rectangular distribution suggested by Brinch and Hansen (1961) seems to hold promise for piles in clay. The magnitude of the pressure can be computed from the suggested earth pressure coefficients (Meyerhof *et al.* 1981). The lateral soil pressures under working loads at intermediate inclinations and eccentricities can approximately be predicted. It is interesting to note

that considerable lateral pressures are induced on displacement piles jacked into clay.

Even though the present tests have indicated the propriety of the proposed methods for estimating the lateral soil pressures, pile capacity and toe resistance, it is strongly felt that adequate field testing should be undertaken to verify the predictions.

### Acknowledgements

The research at the Technical University of Nova Scotia was carried out with the financial support of the Natural Science and Engineering Research Council of Canada. The leave granted to V.V.R.N. Sastry by the Osmania University of Hyderabad, India is gratefully acknowledged. The assistance provided by Nolan, Davis and Associates, Halifax, in drafting the figures and typing the manuscript is also acknowledged.

### References

- ADAMS, J.J. and RADHAKRISHNA, H.S., (1973) : "The lateral capacity of deep augered footings." *Proc. of 8th Int. Conf. on Soil Mechanics and Found. Eng.*, Moscow, Vol. 2. 1 : 1-8.
- BRIAUD, J.L., SMITH, T., and MEYER, B., (1983) : "Pressuremeter gives elementary model for laterally loaded piles." *Symposium of International Insitu Testing*, Paris. 2 : 217-221.
- BRINCH HANSEN, J., (1961) : "The ultimate resistance of rigid piles against transversal forces." Bulletin No. 12, *Danish Geotechnical Institute, Copenhagen*.
- BROMS, B.B., (1964) : "Lateral Resistance of piles in cohesive soils." *ASCE Soil Mech. and Found. Eng. Div.*, 90 : SM 3 : 123-56.
- BROMS, B.B., (1964) : "Lateral Resistance of piles in cohesive soils." *ASCE, Soil Mech. and Found. Eng. Div.*, 90 : SM 2 : 27-63.
- CHARI, T. R. and MEYERHOF, G.G., (1983) : "Ultimate capacity of rigid single piles under inclined loads in sand." *Canadian Geotechnical Journal*, 20 : 849-854.
- KERISEL, J., and ADAM, M., (1967) : "Calcul des forces horizontales applicables aux fondations profondes dans les argiles et limons." *Supplement, Annales de de L'institut Technique du Batiment et des Travaux Publics*, Paris, No. 239 : 1655-1693.
- KIRBY, R.C., and ESRIG, M.I., (1980) : "Furtner development of a general effective stress method for prediction of axial capacity for driven piles in clay. Recent developments in the design and construction of piles." *Inst. of Civil Engs.* London, pp 335-344.
- KOUMOTO, T., MEYERHOF, G.G., and SASTRY, V.V.R.N., (1986) : "Analysis of bearing capacity of rigid piles under eccentric and inclined loads." *Canadian Geotechnical Journal*, Vol. 23, No. 2.

MEYERHOF, G.G., (1972) : "Stability of slurry trench cuts in saturated clay". *Proc., Speciality Conf. on the Performance of Earth and Earth Supported Structures.* Purdue University, 1, 1451-66.

MEYERHOF, G.G., (1976) : "Bearing capacity and settlement of pile foundations." ASCE, *Journal of the Geotechnical Engineering Division*, 102 : GT3 : 195-228.

MEYERHOF, G.G., and HANNA, A.M., (1978) : "Ultimate bearing capacity of foundations on layered soils under inclined load." *Canadian Geotechnical Journal*, 15 : 4 : 565-572.

MEYERHOF, G.G., and MATHUR, S.K., and VALSANGKAR, A.J., (1981) : "Lateral resistance and deflection of rigid walls and piles in layered soils." *Canadian Geotechnical Journal*, 18 : 159-70.

MEYERHOF, G.G., and RANJAN, M., (1972) : "The bearing capacity of rigid piles under inclined loads in sand, 1. Vertical piles." *Canadian Geotechnical Journal*, 9 : 430-446.

MEYERHOF, G.G., and SASTRY, V.V.R.N., (1985) : "Bearing capacity of rigid piles under eccentric and inclined loads." *Canadian Geotechnical Journal*, 22, 3 : 267-276.

MEYERHOF, G.G., and YALCIN, A.S., (1984) : "The bearing capacity of rigid loads in clay." *Canadian Geotechnical Journal*, 21 : 3 : 389-96.

MEYERHOF, G.G., and YALCIN, A.S., and MATHUR, S.K., (1983) : "Ultimate pile capacity for eccentric inclined load." ASCE, *Journal of the Geotechnical Division*, 109 TG 3 : 408-23.

SASTRY, V.V.R.N., (1977) : "*Bearing capacity of piles in layered soil.*" Ph. D. Thesis, Technical University of Nova Scotia, Halifax, N.S.

SASTRY, V.V.R.N., and MEYERHOF, G.G., (1986) : "Lateral soil pressures and displacements of rigid piles in homogeneous soils under eccentric and inclined loads". *Canadian Geotechnical Journal*, 23 : (in press) .

TERZAGHI, K., (1943) : "*Theoretical Soil Mechanics.*" New York, John Wiley and Sons, New York.

## Notation

$A_p$	= area of pile point
$A_s$	= area of pile shaft
$B$	= pile width
$C_1, C_2$	= soil adhesion on pile shaft
$C_u$	= uniformity coefficient
$c_u$	= undrained shear
$D$	= depth
$D_{10}$	= effective size
$D_r$	= relative density
$E_s$	= secant modulus of soil
$e$	= eccentricity of load

$F$	= factor of safety
$i_c, i_\gamma$	= inclination factors for pile point resistance in clay and sand respectively
$K_b$	= pile shape factor for lateral earth pressure in sand
$K_c$	= pile shape factor for lateral earth pressure in clay
$K_o$	= coefficient of earth pressure at rest
$K_s$	= coefficient of earth pressure on shaft
$M_o$	= pile capacity under pure moment
$M_u$	= moment on the pile due to eccentric load at failure
$m$	= coefficient
$N_q$	= bearing capacity factor
$P_1, P_2$	= earth thrusts
$Q$	= total load on pile
$Q_o$	= pile capacity under axial load
$Q_{90}$	= pile capacity under horizontal load
$Q_p$	= point resistance of pile
$Q_u$	= total load on pile at failure
$r$	= adhesion factor
$S$	= degree of saturation
$W$	= liquid limit
$W_p$	= plastic limit
$W_n$	= water content
$\alpha$	= inclination of load with vertical
$\gamma$	= unit weight of soil
$\delta, \delta_1, \delta_2$	= angles of skin friction
$\delta_3$	= inclination of $Q_p$ with vertical
$\sigma$	= net lateral soil pressure at any depth
$\sigma_a$	= lateral soil pressure decrease due to load on pile in clay
$\sigma_b$	= net lateral soil pressure at pile base at failure
$\sigma_i$	= lateral soil pressure due to pile installation
$\sigma_p$	= lateral soil pressure increase due to load on pile in clay
$\sigma_u$	= net lateral soil pressure at any depth at failure
$\phi_p$	= angle of internal friction in plane strain
$\phi_t$	= angle of internal friction from triaxial test
$\eta$	= porosity
$\theta$	= equivalent inclination of load